Recent Studies of Shubing Dai's Group

Shubing Dai

Northwest A&F University
Yangling, Shaanxi , China

20/02/2024, A Coruna,Spain

CONTENTS

Summary of Recent Papers:

1.Shubing Dai, Shuya Yang, Yuchen Zhang, Xiang He, Ziren Li, Kuandi Zhang, Jingming Hou, Dongpo Wang, Jijian Yang, Yang Xue, Sheng Jin, Yu Li.Numerical study of impact pressure and force of **cascading dam-break** floods on the downstream dam. ***(Under Review)***

2.Shubing Dai, Jian Hou, Sheng Jin, Kuandi Zhang, Jingming Hou, Gang Liu. Discharge coefficients formulae of **grate inlets** of complicated conditions for urban floods simulation and urban drainage systems design. ***Journal of Hydrology***,*2023, 625(1):130089.*

3.Shubing Dai, Xinyuan Liu,Kuandi Zhang, Yulei Ma, Hansheng Liu, Sheng Jin. Numerical study of **roll wave** development for non-uniform initial conditions using steep slope shallow water equations. ***Physics of Fluids***, *36(2),2024.*

PART 01

Numerical Simulations Impact Pressure and Force of Cascading Dam Break Floods on the Downstream Dam

Shubing Dai et al.2024 (Under Review)

01 Research background

Fig. 5(a) Two-stage cascading dam-breaks, Derna, Libya, 20000 deaths, 2023.9 (Marshall. Nature, 2023)

Fig. 5(b) 60-stage cascading dam-breaks, Henan, China, 200000 deaths, 1975.8 (Xu. 2013)

Fig. 5(c) 4-stage cascading dams downstream of Jinshajiang River, China, all are top eight hydropower stations in the world

These cascading dams subject to external factors poses a potential catastrophic consequence of dam-break floods.The water in the upstream reservoir rushes downstream, causing extensive damage to downstream areas and even the potential failure of cascading reservoirs. This study offers valuable scientific guidance and technical support for disaster prevention and mitigation strategies concerning cascading dam-break floods.

02 Experimental Methods

The dam-break phenomenon was simulated in the laboratory. The evolution of dam-break waves and their interaction with structures under different inflow, initial water depth ratio, bottom slope and steep overcurrent structure conditions were studied. The equipments required for the experiment diagram are as follows.

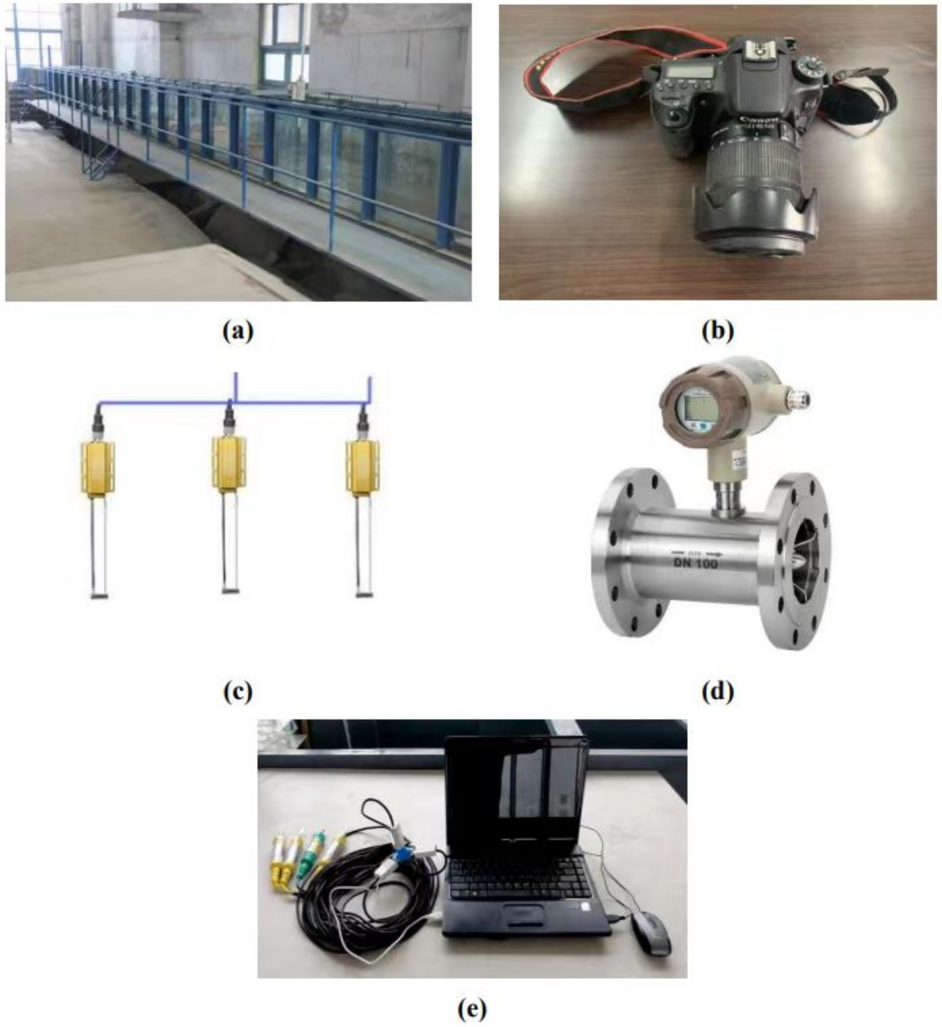

Fig.6 Experimental device.

02 Experimental Materials and Methods

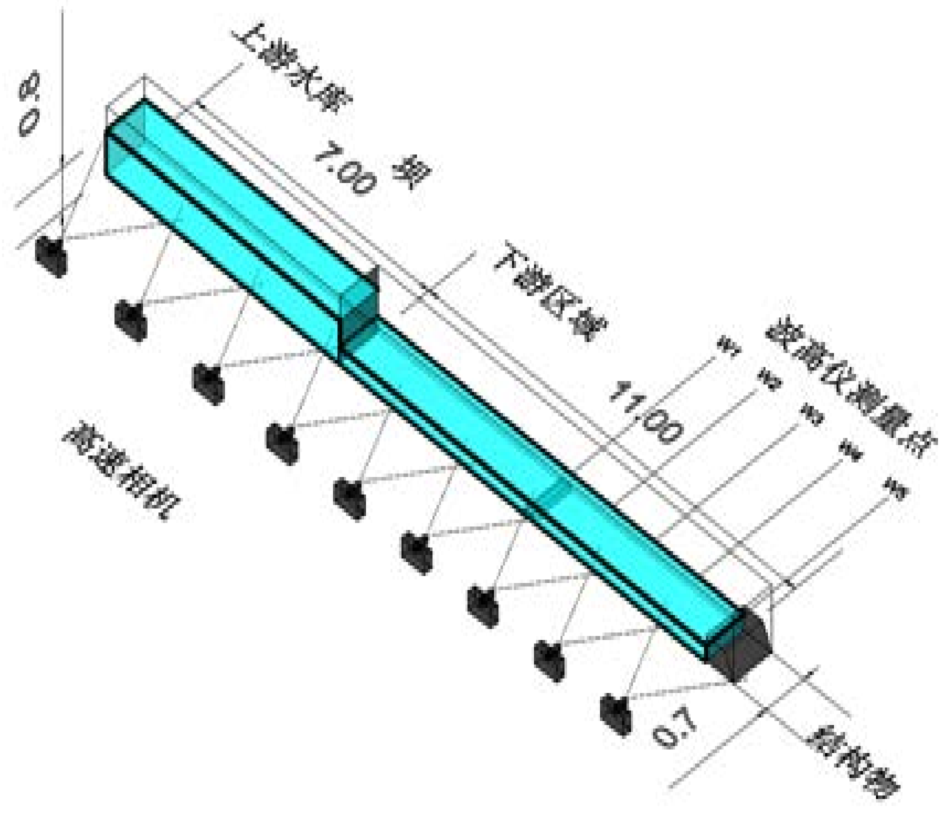

Fig.7 The schematic diagram.

The experiment of cascading dam-break floods will be conducted in the laboratory. The evolution of dam-break waves and their interaction with downstream structures and dams under different inflow, initial water depth ratio, bottom slope will be studied.

03 Research findings

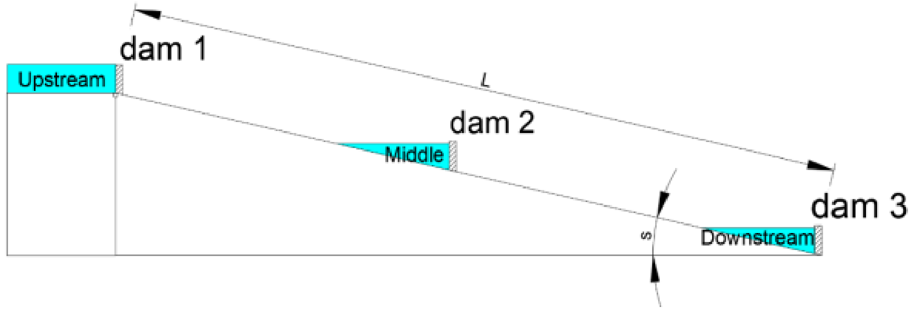

(a) Three-stage cascading dam-break

Fig.8 3-stage Cascading Dam-break Floods Benchmark

Firstly, a shallow water model based on MUSCL-Hancock Finite-volume method was developed to conduct the study.

$$\mathbf{U}_{i,j}^{n+1} = \mathbf{U}_{i,j}^{n} - \frac{\Delta t}{\Delta x}(\mathbf{F}_{i+1/2,j} - \mathbf{F}_{i-1/2,j}) - \frac{\Delta t}{\Delta y}(\mathbf{G}_{i,j+1/2} - \mathbf{G}_{i,j-1/2}) + \Delta t\mathbf{S}_{bi}^{n} + \Delta t\mathbf{S}_{fi}^{n}$$

$$\frac{\partial \mathbf{U}}{\partial t} + \frac{\partial \mathbf{F}}{\partial x} + \frac{\partial \mathbf{G}}{\partial y} = \mathbf{S}_b + \mathbf{S}_f,$$

$$\mathbf{U} = \begin{pmatrix} h \\ hU \\ hV \end{pmatrix}, \mathbf{F} = \begin{pmatrix} hU \\ \beta hU^2 + \frac{1}{2} g\cos^2\theta h^2 \\ \beta hUV \end{pmatrix}, \mathbf{G} = \begin{pmatrix} hV \\ \beta hUV \\ \beta hV^2 + \frac{1}{2} g\cos^2\theta h^2 \end{pmatrix},$$

$$\mathbf{S}_b = \begin{pmatrix} 0 \\ -g\cos^2\theta h\dfrac{\partial z_b}{\partial x} \\ -g\cos^2\theta h\dfrac{\partial z_b}{\partial y} \end{pmatrix}, \mathbf{S}_f = \begin{pmatrix} 0 \\ -\dfrac{g\cos^2\theta n^2 U\sqrt{U^2+V^2}}{h^{1/3}} \\ -\dfrac{g\cos^2\theta n^2 V\sqrt{U^2+V^2}}{h^{1/3}} \end{pmatrix}$$

where **U** is vector of conserved variables; **F** and **G** are flux vectors in the *x* and *y* directions; $\mathbf{S}_b$ is bed slope source term vector; $\mathbf{S}_f$ is friction source term vector; *h* is water depth; *U* and *V* are depth-averaged velocity in the *x* and *y* directions; β is the correction factor for the non-uniform vertical velocity profile, which equals 1.016 when a seventh power law velocity distribution is assumed (Liang et al. 2006); *g* is gravity acceleration; θ is the slope angle of the bed; z_b is the bed elevation; *n* is Manning coefficient.

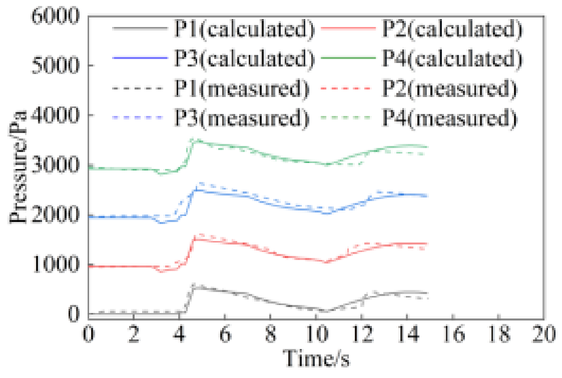

（a） ho=0.1m, hd=0.3m,L=5m

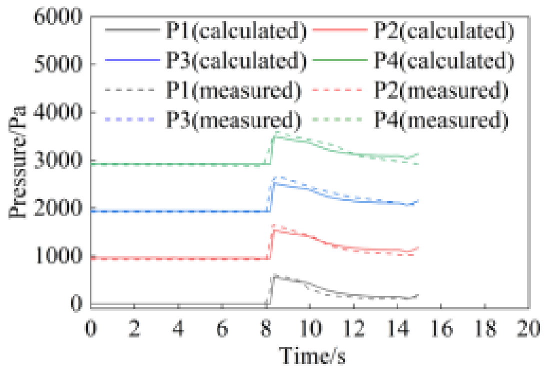

（b） ho=0.1m, hd=0.3m,L=10m

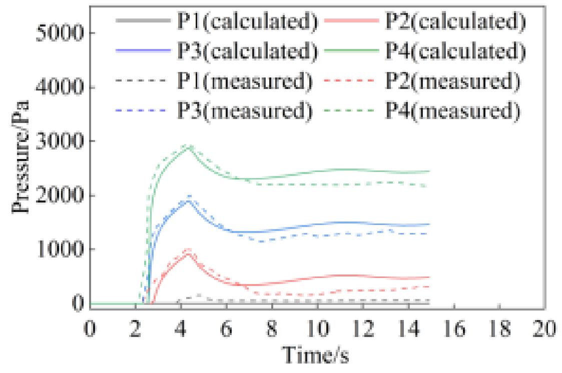

（c） ho=0.25m, hd=0m,L=5m

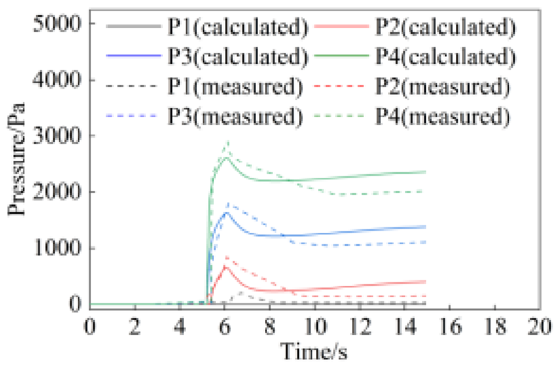

（d） ho=0.25m, hd=0m,L=10m

Fig.9 Comparisons of the measured and calculated pressure history of 4 runs for S = 4°

Fig.9 shows the comparisons of the impact pressures calculated by the numerical model with and withoutt considering the bed slope. It can be seen that the calculated results of the two numerical models are basically consistent, which are in good agreement with the measured results.

03 Research findings

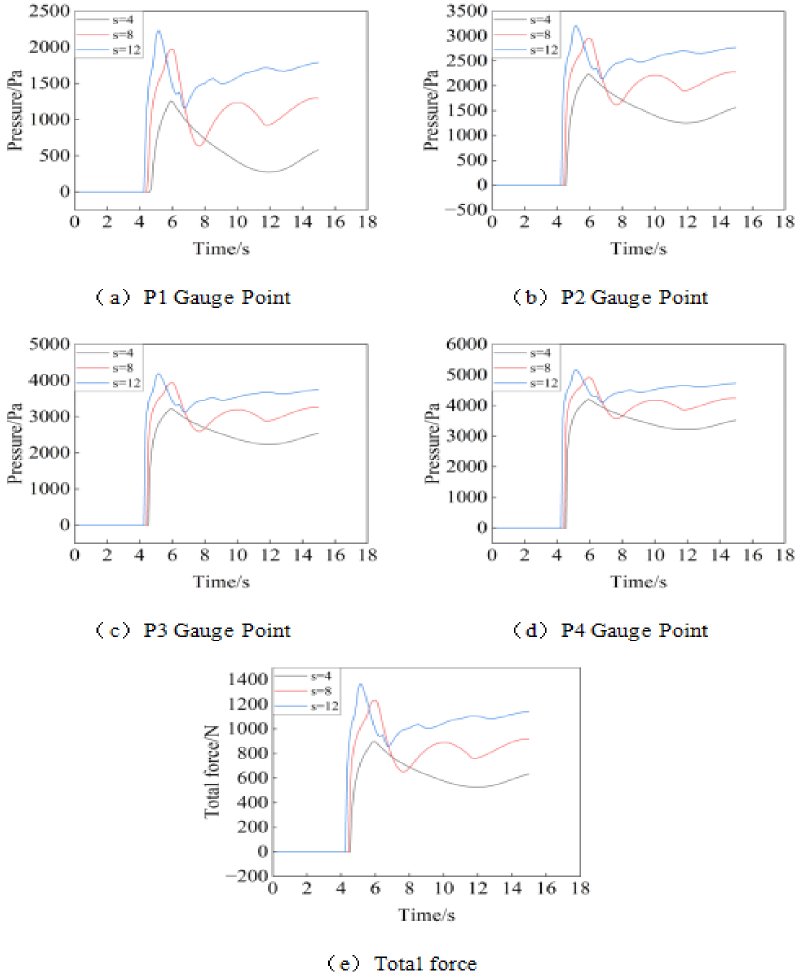

Fig. 10 shows that for the same volume of water in the downstream reservoir, steeper bed slopes result in higher impact pressure and force, and earlier impact time.

Fig.10 The impact pressure history of 4 gauge points and impact force history for different bed slopes.

02 Research findings

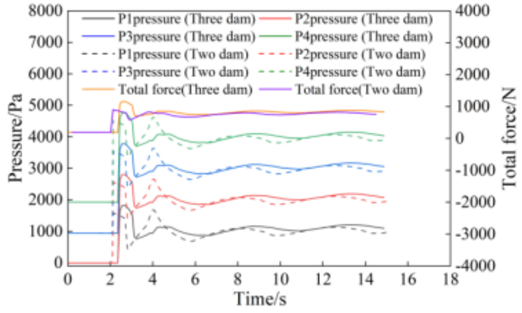

(a)ho=0.25m,hm=0.1m,hd=0.2m, L=5m

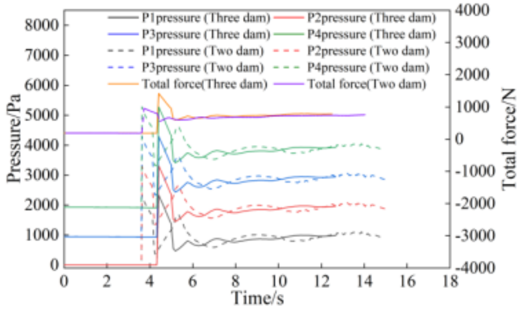

(b)ho=0.25m,hm=0.1m,hd=0.2m, L=10m

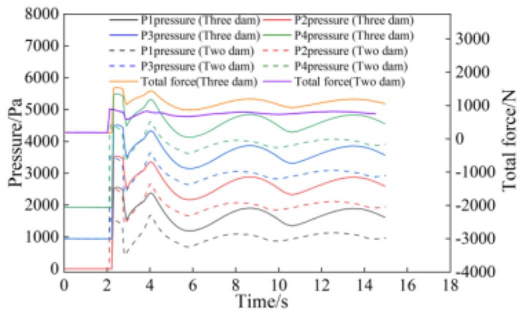

(c)ho=0.25m,hm=0.25m, hd=0.2m,L=5m

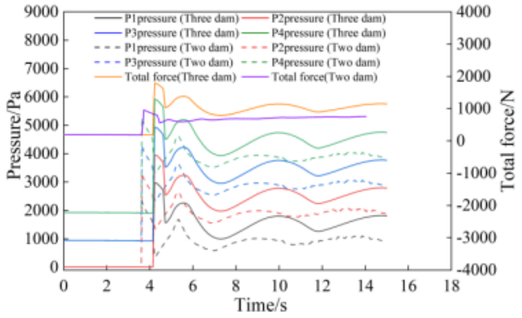

(d)ho=0.25m,hm=0.25m,
hd=0.2m,L=10m

Fig.11 Comparisons of impact pressure of 4 gauge points and impact force of two-stage and three-stage dam-break for S =8°.

Because many parameters will affect the pressure at each point, this paper comprehensively analyze the effects of slope, dam spacing, water depth, etc., on the impact pressure and force on the downstream dam .

It can be seen from **Fig. 11** that three-stage dam-break have larger pressure and force peaks than two-stage dam-break, and the impact time of the former one is still later.

04 Discussion and Conclusion

I

Keeping all the other parameters consistent, the larger the dam spacing, the greater the peak value and average value of the impact pressure and force on the downstream dam surface, and the later the impact time of the dam-break wave.

II

The water depths of the upper, middle and lower reaches have an effect on the pressure at each point.

III

Under different bed slope conditions, with the decrease of slope degree, the impact peak pressure and force of each measuring point gradually decreases, the impact time delays.

IV

The impact time of the dam-break flood on the downstream dam surface after the three-stage dam-break is slightly later than that of the two-stage dam-break. The peak and average values of the impact pressure and force caused by the three-stage dam break are higher than those of the two-stage dam break.

PART 02

Discharge Coefficients Formulae of Grate Inlets of Complicated Conditions for Urban Floods Simulation and Urban Drainage Systems Design

Journal of Hydrology

Shubing Dai et al. Journal of Hydrology,2023, 130089.

01 Research background

Fig.12 Urban floods (a)urban drainage of grate inlets; (b)flooding; (c) intrusion into subway.

Global warming and accelerated urbanization process results in severe urban floods all over the world.The grate inlet is a key element for the exchange of surface water flow and underground drainage network flow in urban floods.Quantifying the exchange discharge of grate inlets plays an important role in the simulation of urban floods and design of sustainable urban drainage systems.

02 Experimental Materials and Methods

Fig.13 Experimental platform in Dalian University of Technology, China

A rectangular channels with adjustable horizontal and vertical slopes to simulate the real road surface in urban areas.The channel is 7 meters long, 2.33 meters wide, and 0.15 meters deep. The right side of the channel is equipped with grate inlets and slots for experiments.

03 Research findings

The following formula was used to calculate the discharge coefficient of the grate inlets:

$$m = \frac{Q}{1000 * \sqrt{2g} * (h + \frac{v^2}{2g})^{1.5} * L} \qquad (1)$$

Due to many influencing parameters of discharge coefficient, this work will comprehensively compare and analyze all parameters, mainly using the above formula to analyze the relation among discharge Q, discharge coefficient m, and all remaining influencing parameters Q/m, as shown in the figure on the right.

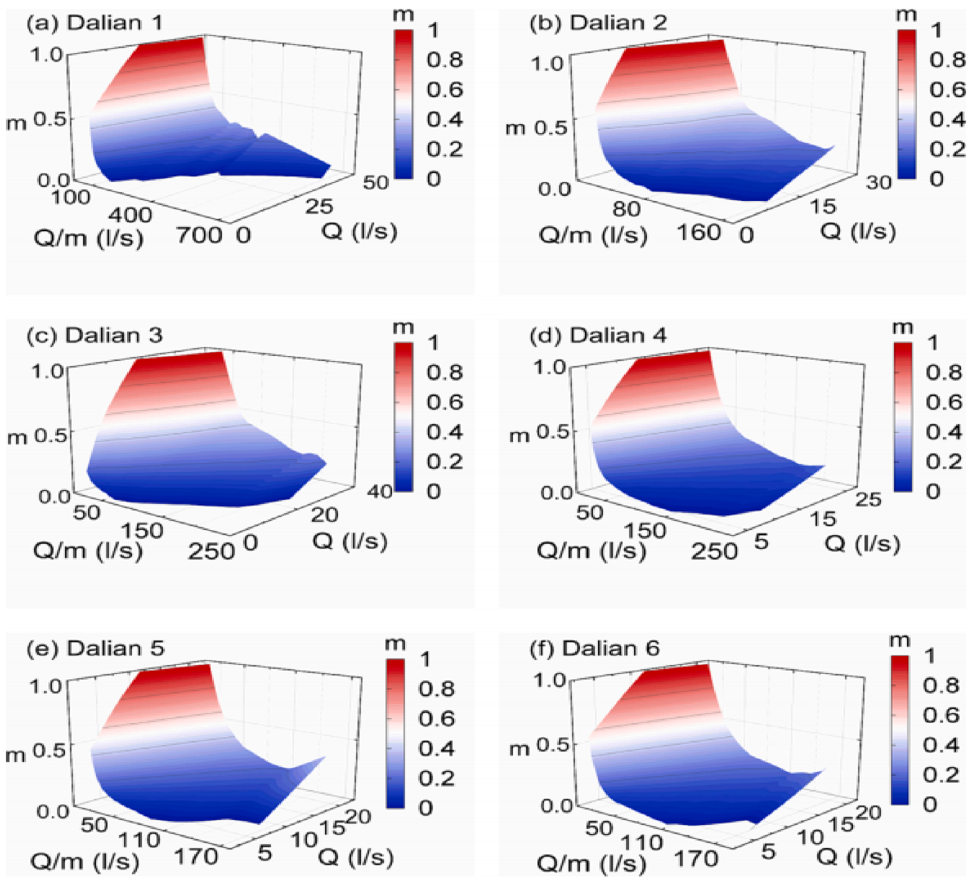

Fig. 2. The three-dimensional relationship between the discharge coefficient m and the product Q/m of the interception discharge Q and all remaining influencing parameters for different grate inlets.

Fig.14 The relationship among Q, m and Q/m.

03 Research findings

Based on the Buckingham's theorem of dimensional analysis, the general relationship between the discharge coefficient of grate inlets and other effective influencing parameters:

$$\pi_1 = \frac{nb}{B} \qquad \pi_6 = \frac{v}{\sqrt{gB}}$$

$$\pi_2 = \frac{kl}{B} \qquad \pi_7 = \frac{h}{B}$$

$$\pi_3 = \varepsilon \qquad \pi_8 = \frac{w}{B}$$

$$\pi_4 = S \qquad \pi_9 = \frac{\mu}{\rho B\sqrt{gB}}$$

$$\pi_5 = i \qquad \pi_{10} = \frac{\sigma}{\rho g B^2}$$

In this study, the discharge coefficients of parallel and vertical water grates were considered in the following nonlinear regression form:

$$m = c_1 + c_2\left(\frac{nb}{B}\right)^{c_3} * \left(\frac{kl}{B}\right)^{c_4} * (\varepsilon)^{c_5} * (S)^{c_6} * (i)^{c_7} * (Fr)^{c_8} * \left(\frac{h}{nb}\right)^{c_9} * \left(\frac{w}{B}\right)^{c_{10}} * (Re)^{c_{11}} * (We)^{c_{12}} \qquad (2)$$

03 Research findings

We can obtain 12 sets of discharge coefficient calculation formulas for a series of parallel and vertical grate inlets, but we only list 6 sets here.

Formulae for parallel grate inlets:

$$m = -0.06008669 + 0.2859835 * (\frac{nb}{B})^{-0.3374040} * (\frac{kl}{B})^{0.1227811} * (\varepsilon)^{0.3787224} * (S)^{0.2597921} * (i)^{-0.04520118} * (Fr)^{-1.247524} * (\frac{h}{nb})^{-0.5647858} * (\frac{w}{B})^{-0.2917848} * (Re)^{-0.009536341} * (We)^{-0.1377968} \quad (3)$$

$$m = -0.1029380 + 3.110816 * (\frac{nb}{B})^{0.2870714} * (\varepsilon)^{1.019732} * (Fr)^{-0.9262511} * (\frac{w}{B})^{-0.3858472} \quad (4)$$

$$m = -0.03625441 + 3.749670 * (\varepsilon)^{1.166577} * (Fr)^{-1.215834} \quad (5)$$

Formulae for vertical grate inlets:

$$m = -0.1451635 + 0.8531193 * (\frac{nb}{B})^{0.2685055} * (\frac{kl}{B})^{0.2587059} * (\varepsilon)^{0.2118278} * (S)^{0.1513753} * (i)^{-0.09472032} * (Fr)^{-0.9927507} * (\frac{h}{nb})^{-0.3233670} * (\frac{w}{B})^{-0.6553513} * (Re)^{-0.01691412} * (We)^{0.006173829} \quad (6)$$

$$m = -0.1786434 + 1.043489 * (\frac{kl}{B})^{0.4672118} * (Fr)^{-1.009400} * (\frac{h}{nb})^{-0.1968524} * (\frac{w}{B})^{-0.3166776} \quad (7)$$

$$m = 0.06988001 + 2.708673 * (Fr)^{-2.666045} \quad (8)$$

The influencing parameters of the formula change from more to less, and R^2 gradually decreases as well.

03 Research findings

Fig. 15 shows the comparisons between the calculated values and the measured values of each group of formulas for the calibration and validated runs.

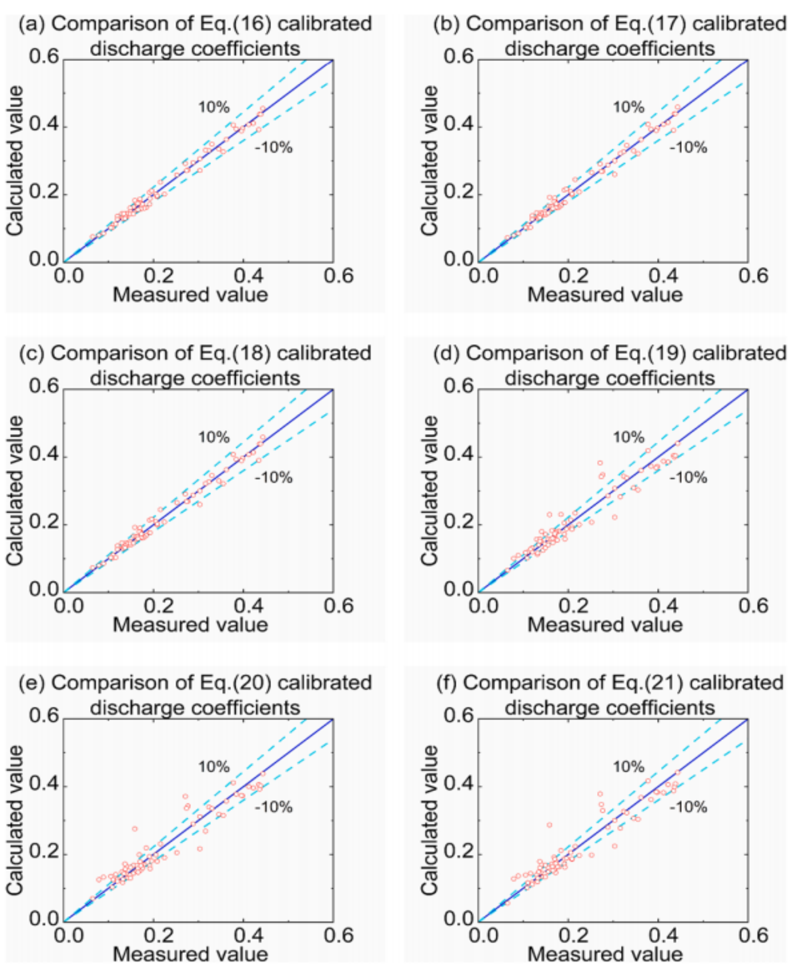

Fig. 5. Comparison between the calculated values of the discharge coefficient calibration equation and the measured values of the calibration series for parallel grate inlets.

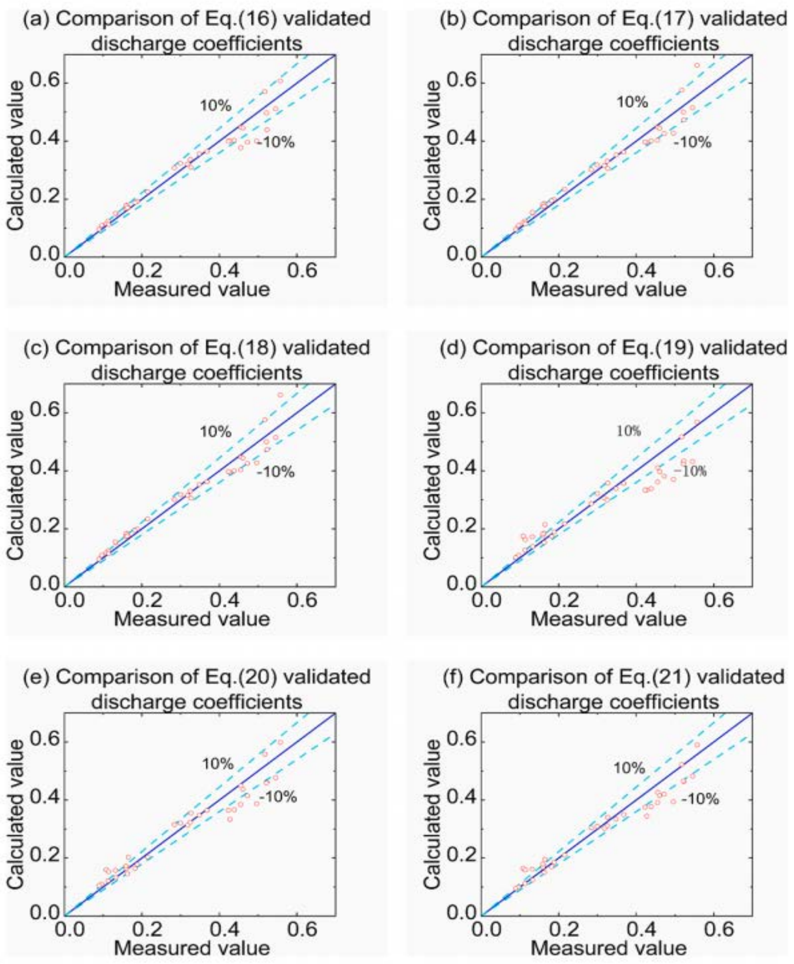

Fig. 6. Comparison between the calculated values of the discharge coefficient calibration equation and the measured values of the validation series for parallel grate inlets.

Fig.15 Comparisons between the calculated discharge coefficients and measured ones.

03 Research findings

We also conducted a detailed study on the relationship between the discharge coefficient and the approaching Froude number of six grate inlets. When the Froude number increases, the discharge coefficient decreases.The R^2 of parallel grates is greater than that of vertical grates, indicating that the discharge capacity of parallel grate inlets is more closely related to the Froude number.

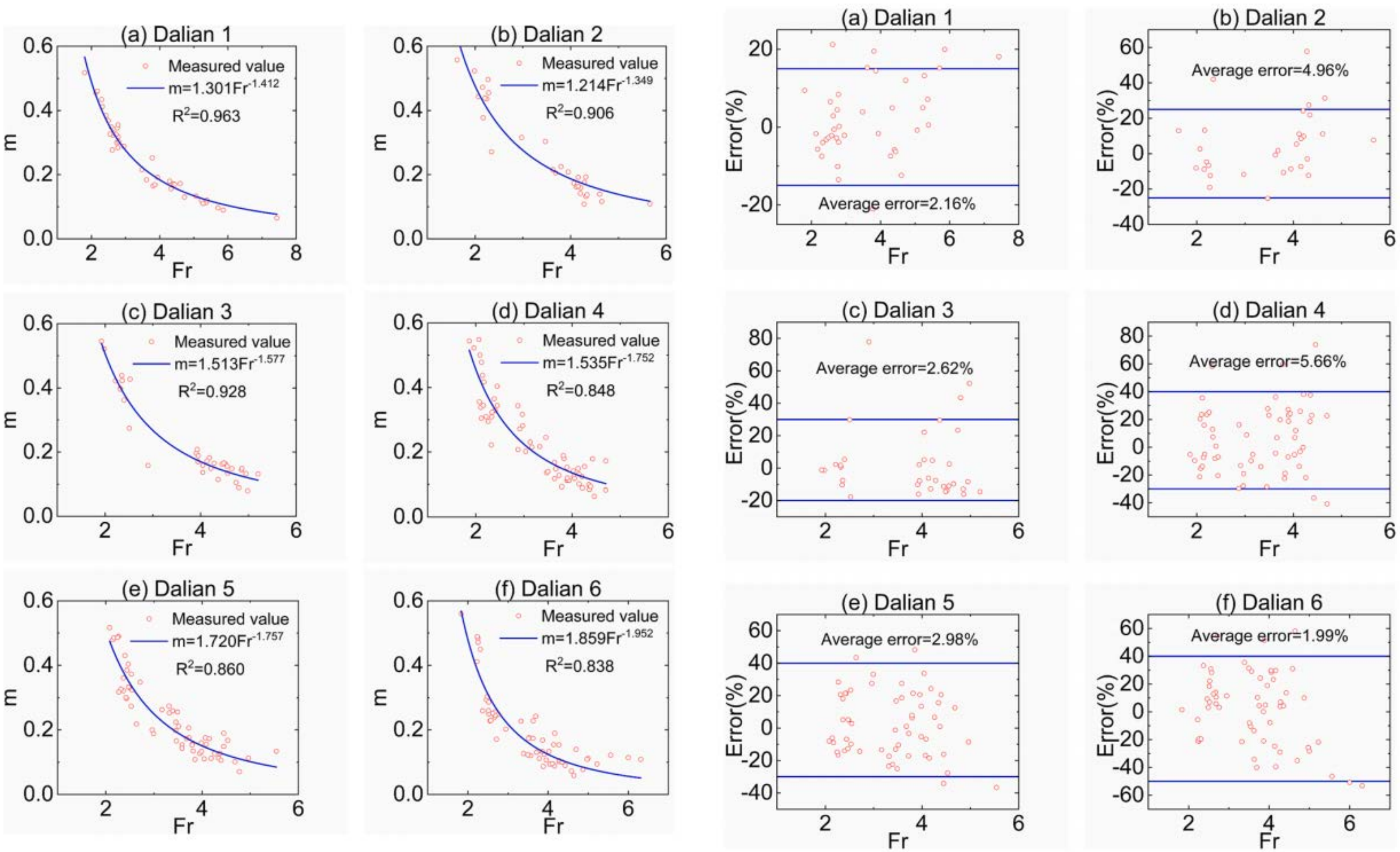

Fig.16 The relationship between the discharge coefficients and approaching Froude number.

03 Research findings

We use previously published experimental data to verify that there is a clear power function relationship between discharge coefficient m and Fr, which is similar to the research results in our paper. This further indicates that the research results in this paper have accuracy and generality.

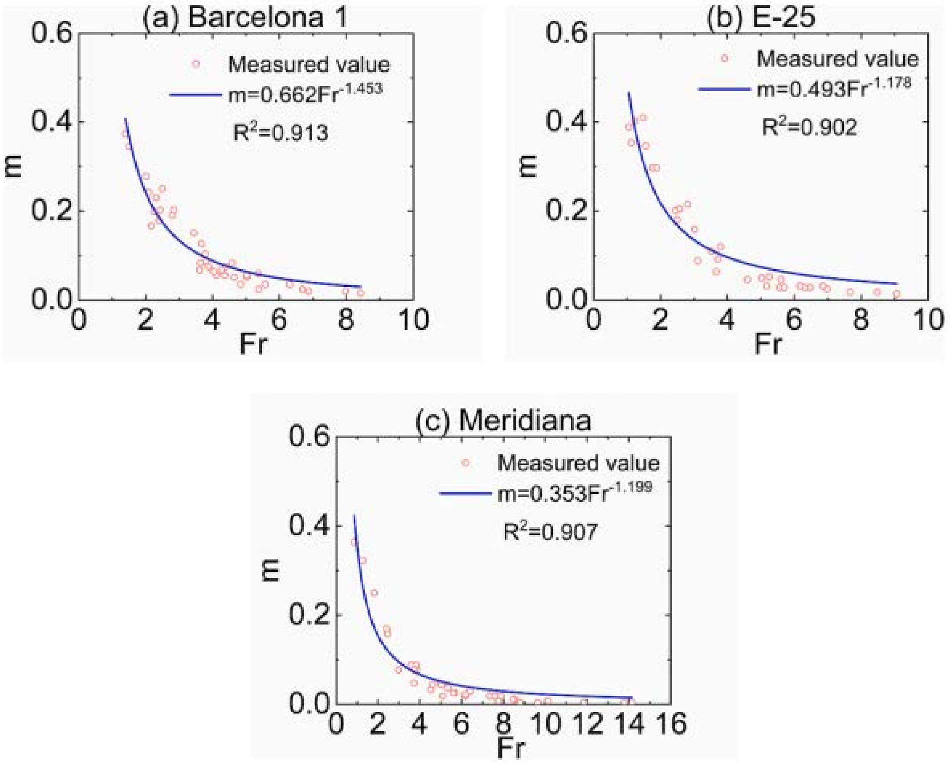

Fig.17 The relationship between the discharge coefficients and approaching Froude number for published experimental data (Cosco et al. 2020).

04 Discussion and Conclusion

Ⅰ

For the same other parameters, as the Q increases, the discharge coefficient also increases. When the Froude number increases, the discharge coefficient decreases. The performance of parallel grate inlets and vertical grate inlets in terms of discharge coefficient is not significantly different.

Ⅱ

Using the Buckingham's theorem of dimensional analysis, 12 sets of precise formulas for calculating the discharge coefficient of grate inlets were proposed. These 12 sets of formulas have clear physical meanings and high accuracy, with an average relative error between 0.37% and 5.41%;

Ⅲ

Strong correlation between the discharge coefficient of the grate inlet and the Froude number of the approaching flow was observed.

Ⅳ

In order to improve the discharge capacity of grate inlets, the hole width and length should be appropriately increased to increase the porosity of the grates, and the transverse slope should be increased as much as possible, while the longitudinal slope should be reduced to increase drainage capacity. Under supercritical conditions, reducing the Froude number through appropriate measures can increase the drainage capacity of grate inlets, such as increasing road roughness.

PART 03

Current Progress of Experimental and Numerical Study of Exchange of Surface and Sewer Flow for Urban Floods

A new urban flood experiment platform considering the sewer network is being built, which is located in the Engineering Hydraulics Laboratory of the School of Water Resources and Architectural Engineering, Northwest A&F University.

(1)The top image shows the experimental urban road using a rectangular channel with adjustable horizontal and longitudinal slopes. The left side of the channel is equipped with grate inlets and slots for experiments, and different geometric parameters of grate inlets can be installed as needed.

(2)The below image is integrated platform with road surface and underground sewer network, which can simulate the interaction between surface water flow and sewer flow.

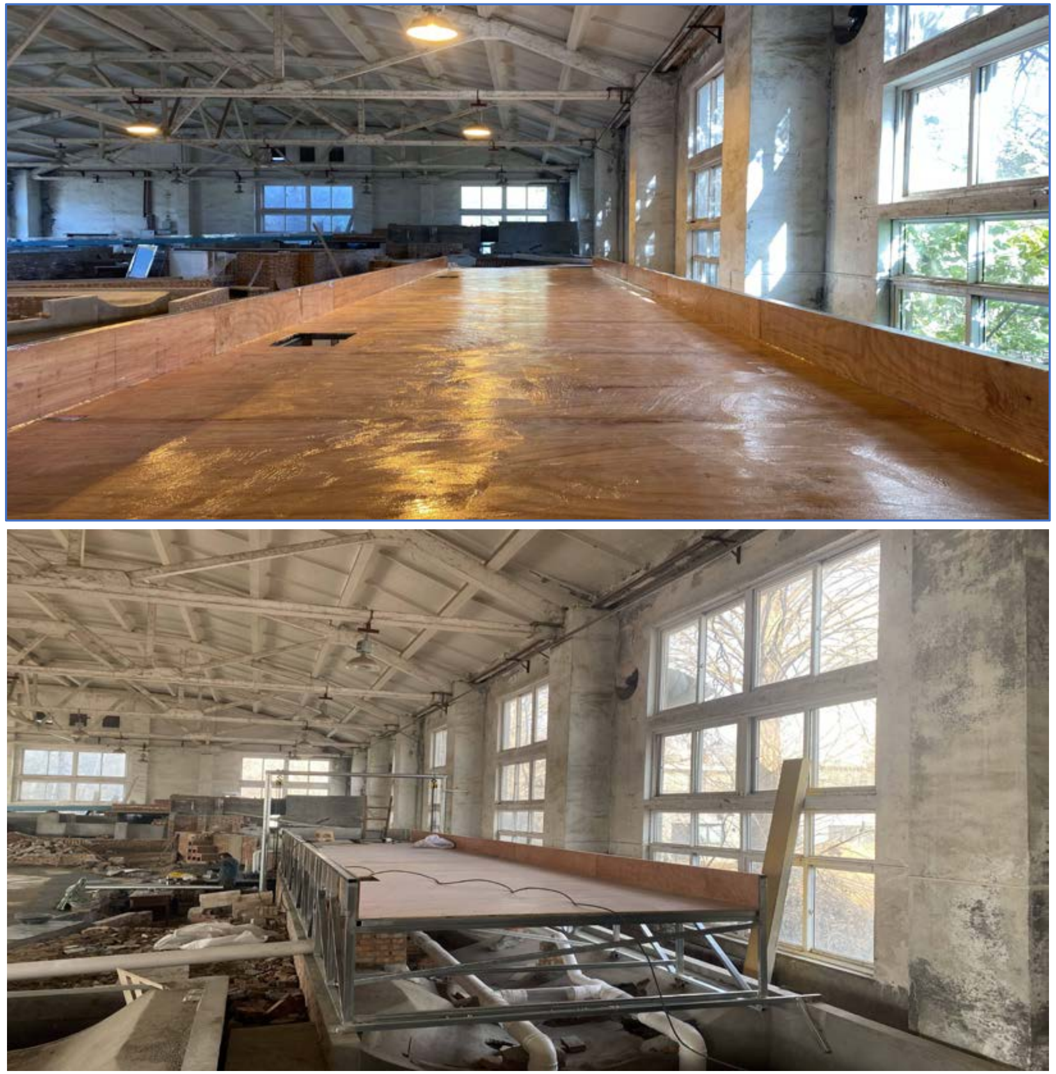

Fig.18 New experimental platform of urban floods considering sewer network.

Currently, I am using the dual drainage model Iber-SWMM to study the exchange discharge of grate inlets by implementing the formulae (20) in our paper (only considering Froude number and void rate) into the codes of subroutine interchange_2D1D_inlets. Primary results have been obtained, showing good agreements between experimental and calculated exchange discharges. Some limitation exists in this version due to the formulae focusing on supercritical flow conditions. In the near future, we will obtain some other accurate formulae of different grate inlets considering subcritical and supercritical flow, surcharging flow and vice versa. As well, we expect to do some wash-off experiments on the new platform by rainfall simulator, to study the exchange of sediment and pollutants.

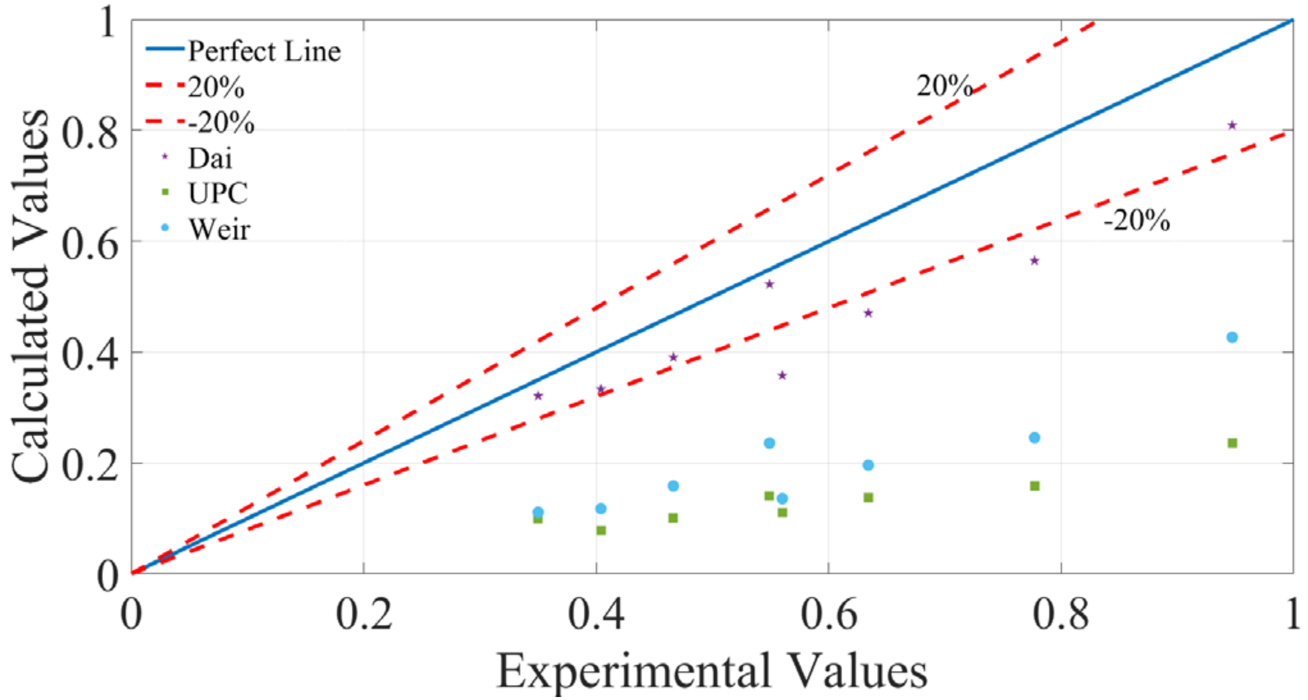

Thanks for your attention!

Whatsapp:+34 617348083

Email:daishubing1990@nwafu.edu.cn